Front. Earth Sci. 2023, 17(3): 856−866
https://doi.org/10.1007/s11707-022-1039-5

RESEARCH ARTICLE

Effect of permeability and its horizontal anisotropy on enhanced coalbed methane recovery with CO_2 storage: quantitative evaluation based on staged CH_4 output inhibition

Ziliang WANG[1,2], Shuxun SANG (✉)[3,4], Xiaozhi ZHOU (✉)[1,2], Xudong LIU[1,2], Shouren ZHANG[5]

1 Key Laboratory of Coalbed Methane Resources & Reservior Formation Process (Ministry of Education), China University of Mining and Technology, Xuzhou 221008, China
2 School of Resources and Geosciences, China University of Mining and Technology, Xuzhou 221008, China
3 Carbon Neutrality Institute, China University of Mining and Technology, Xuzhou 221008, China
4 Jiangsu Key Laboratory of Coal-Based Greenhouse Gas Control and Utilization, Xuzhou 221008, China
5 China United Coalbed Methane Co. Ltd. (CUCBM), Beijing 100011, China

Abstract The permeability and its horizontal anisotropy induce a critical influence on staged CH_4 output inhibition process. However, a quantitative evaluation of this influence has been rarely reported in the literature. In this work, the impact of horizontal anisotropic permeability on CO_2-ECBM was numerically investigated. The variation in the staged CH_4 output inhibition was analyzed. The ideal displacement profile of the CO_2-ECBM process was established for the first time. Moreover, the variation in CH_4 output of different wellbores was discussed. The results showed that 1) low-permeable or weak-anisotropic reservoirs were not conducive to enhanced CH_4 recovery owing to long inhibition time (> 1091 days) and high inhibition level (> 36.9%). As permeability and anisotropy increased, due to the accelerated seepage of free water, the hysteresis time and inhibition time could decrease to as short as 5 days and 87 days, respectively, and the inhibition level could weaken to as low as 5.00%. Additionally, the CH_4 output and CO_2 injection could increase significantly. 2) Nevertheless, high permeability and strong anisotropy easily induced CO_2 breakthrough, resulting in lower CH_4 production, CO_2 injection and CO_2 storage than expected. While maintaining high efficiency of CO_2 storage (> 99%), upregulating CO_2 breakthrough concentration from 10% to 20% might ease the unfavorable trend. 3) Along the direction of fluid flow, the ideal displacement profile consisted of CO_2 enriched bank, CO_2 and CH_4 mixed bank, CH_4 enriched bank, and water enriched bank, whereas a remarkable gap in the displacement profiles of the dominant and non-dominant seepage directions was observed. 4) The potential of CH_4 output might vary greatly among different wellbores. The producers along the dominant seepage direction held more potential for CH_4 recovery in the short-term, while those along the non-dominant seepage direction avoided becoming invalid only if a long-time injection measure was taken for the injectors. These findings pave the way to understand fluid seepage in real complex reservoirs during CO_2-ECBM and conduct further field projects.

Keywords CO_2-ECBM, permeability, anisotropy, the staged CH_4 output inhibition, displacement profile

1 Introduction

Carbon capture, utilization, and storage (CCUS) is an effective technology for achieving carbon reduction (L'Orange Seigo et al., 2014; Hasan et al., 2015; Li et al., 2016; Bui et al., 2018; Tapia et al., 2018; Leonzio et al., 2019). The technology can boost carbon peak and carbon neutrality goals for China (Yu et al., 2019; Jiang et al., 2020; Fan et al., 2021; Sang et al., 2021; Tang et al., 2021; Xu and Dai, 2021; Sun and Chen, 2022). Among various technological solutions, CO_2-ECBM can achieve the dual effect of enhanced CH_4 recovery and CO_2 sequestration by injecting CO_2 into the coal reservoirs, and has attracted more and more attention in recent years

Received April 16, 2022; accepted September 8, 2022

E-mail: shxsang@cumt.edu.cn (Shuxun SANG)
cumtzxz@cumt.edu.cn (Xiaozhi ZHOU)

(White et al., 2005; Godec et al., 2014; Sang, 2018; Vishal et al., 2018; Zhang and Ranjith, 2019). Due to the low permeability, heterogeneity, and anisotropy of coal reservoirs, how to accomplish effective CO_2 injection and efficient CH_4 recovery is a huge challenge for CO_2-ECBM. Currently, the focus is on the reservoir fluid migration process and various of its geological and engineering aspects (Connell and Detournay, 2009; Durucan and Shi, 2009; Kumar et al., 2014; Fan et al., 2019; Liu et al., 2020).

After its injection, CO_2 competes with CH_4 for adsorption. CH_4 desorbs from the microporous surface and diffuses into the coal matrix. Finally, CH_4 percolates in the fracture network and is produced from the wellbore (see Fig. 1) (Godec et al., 2014; Fang et al., 2019a). Scholars have carried out a large number of positive research on these and have reached relatively consistent findings. Increasing the injection pressure and injection rate can improve the CO_2 injection and CH_4 output efficiency, while high pressure and rate will increase the difficulty and technical risks, thus causing premature CO_2 breakthrough (Fan et al., 2019). Permeability is the key element affecting the displacement process (Mazumder and Wolf, 2008; Du et al., 2019; Li et al., 2020; Wang et al., 2021). Good permeability is conducive to great CH_4 output and satisfactory CO_2 sequestration (Pan and Connell, 2011, 2012; Liu et al., 2017). In the CO_2-ECBM process, the permeability is comprehensively affected by effective stress, CO_2 adsorption-induced swelling, CH_4 desorption-induced shrinkage, and Klingenberg effect, showing a decreasing trend on the whole (Fan et al., 2018; Fang et al., 2019b). Kumar et al. (2014) established the heterogeneous permeability distributed in the geometry as a Gaussian normal distribution and studied the effect of CO_2 injection on heterogeneity. Luo et al. (2013) focused on the influence of vertical permeability heterogeneity on CO_2 storage and enhanced CH_4 recovery. Zhao et al. (2020) built the heterogeneous coal model based on computed tomography (CT) and numerical reconstruction, and explored the gas migration process. Despite these studies, little attention has been paid to the effect of horizontal anisotropic permeability on CO_2-ECBM.

In addition, for the evaluation of enhanced CH_4 recovery and CO_2 sequestration, gas driving water has often been ignored, which might lead to the overestimation of CH_4 production. As is well known, during the primary extraction due to free water in the fracture that reduces the gas-phase effective permeability, the coalbed methane migration is impeded in early and intermediate stage (Sun et al., 2018a, 2018b). Just like the primary extraction, the water saturation and gas-phase effective permeability would also change during the gas driving water process in ECBM treatment. Xue et al. (2018) and Kang et al. (2019) found that the content of water decreased after gas flooding and the extraction of water became easier after the treatment. Omotilewa et al. (2021) reported that, during CO_2 injection in the field, the process of gas driving water resulted in an increase in water saturation and a decrease in effective permeability of gas-phase at the displacing front, which led to a slight loss in the production of coalbed methane. Wang et al. (2022) regarded the decrease in gas production caused by gas driving water as the staged inhibition effect on CH_4 output, and initially investigated the influence of permeability on the inhibition process. However, a quantitative evaluation of the influence of anisotropic permeability on the inhibition process has rarely been reported.

In this work, the influence of permeability and its horizontal anisotropy on CO_2 storage and CH_4 output was numerically investigated, and the variation in the staged CH_4 output inhibition resulting from gas driving water was analyzed. Additionally, the ideal displacement profile of the CO_2-ECBM process was constructed for the first time. Finally, the variation in CH_4 output from different wellbores was also discussed. This work is expected to provide some guidance for CO_2-ECBM projects.

2 Methodology

Numerical methods have significant advantages in studying fluid transport processes at an engineering scale, especially in CH_4/CO_2 competitive adsorption and displacement stimulation. In the following sections of the

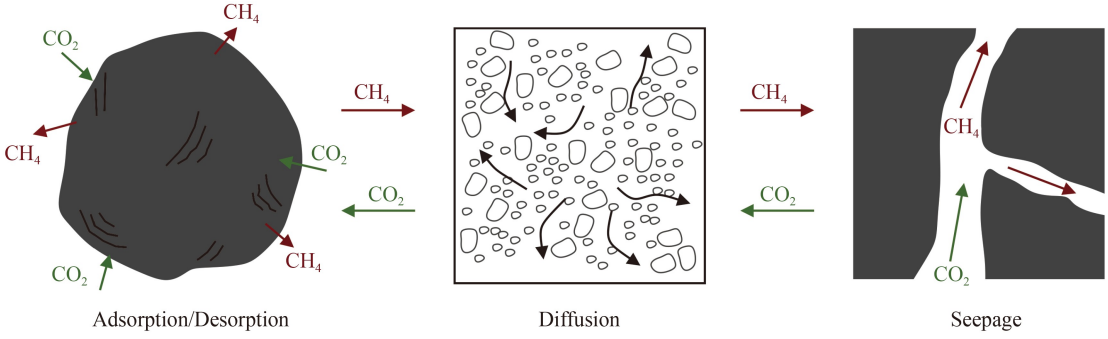

Fig. 1 Microscopic mechanism of CO_2-ECBM gas migration.

study, basic assumptions, governing equations, numerical models, and simulation schemes are explained at length.

2.1 Basic assumptions

The modeling of CO_2 sequestration with enhanced CH_4 recovery was based on the following basic assumptions (Wang et al., 2022). 1) Coal reservoirs can be deemed as a dual-porous medium system consisting of coal matrix and fracture. 2) Gas transportation through the matrix follows Fick's law. 3) Movement of fluid in the coal fracture follows Darcy's law. 4) Coal reservoir remains isothermal, whereas the effect of temperature on the migration of fluid is ignored.

2.2 Governing equations

It is generally believed that coal reservoirs have a double porosity and single permeability system. The fluid flow in the fracture is controlled by the gas mass conservation and water mass conservations, as given by Eq. (1) and Eq. (2) respectively. In Eqs. (1) and (2), P_g and P_w are related to capillary pressure, as given by Eq. (3). Gas and water saturation are given by Eq. (4) (Vishal et al., 2013, 2018).

$$\nabla\cdot[b_g M_g\left(\nabla p_g+\gamma_g\nabla Z\right)+R_{sw}b_w M_w(\nabla p_w+\gamma_w\nabla Z)]_f+q_m+q_g = (\mathrm{d}/\mathrm{d}t)\left(\phi b_g S_g+R_{sw}\phi b_w S_w\right)_f, \quad (1)$$

$$\nabla\cdot[b_w M_w(\nabla p_w+\gamma_w\nabla Z)]_f+q_w=(\mathrm{d}/\mathrm{d}t)(\phi b_w S_w)_f, \quad (2)$$

$$P_{cgw}=p_g-p_w, \quad (3)$$

$$S_g+S_w=1.0. \quad (4)$$

Gas diffusion through coal matrix is determined by Eq. (5).

$$q_{mi}=\frac{V_m}{\tau_i}\left[C_i-C_i(p_i)\right]. \quad (5)$$

2.3 Establishment of the numerical model

The COMET3 software is a 3D, multi-component, gas-water two-phase, triple-porosity (with options of single-porosity and dual-porosity) natural gas development simulator (Paul et al., 1990). The platform can simulate the production and extraction of fluid from conventional reservoirs, as well as coal and shale reservoirs using a quasi-steady and non-equilibrium sorption model (Wei et al., 2015). The dual-porosity model is established on the ideal model of fractured media, as proposed by Warren and Root (Warren and Root, 1963). The gas-water two-phase fluid flows through the fracture system, which can be regarded as continuous. The gas desorbs and diffuses from the discontinuous coal matrix into the fracture system. The two processes are related by the desorption isotherm and diffusion correlation (Vishal et al., 2013). The adsorption of mixed gas conforms to the extended Langmuir isothermal adsorption correlation (Vishal et al., 2018). In addition, the variation of porosity and permeability caused by the changes in reservoir pressure, matrix swelling and shrinkage can be tracked, and the process of enhanced coalbed methane (ECBM) through gas injection can be duplicated in the software (Sawyer et al., 1990; Reeves and Pekot, 2001).

Compared with the COMSOL software, COMET3 owns better computational convergence, especially in solving the two-phase seepage problem, and has been widely applied to engineering problems (Vishal et al., 2013, 2018). Therefore, the platform is adopted in this paper for solving the ECBM problems containing two-phase seepage. An appropriate model consisting of dual-component, dual-porosity, and single-permeability is selected to obtain the solution. Taking a well group with one injector and eight producers as described in Liu et al. (2020) as a reference, the average well spacing of 326.7 m is regarded as the minimum well spacing for the numerical model in this work (Fig. 2(a)). To reduce the calculation time and the computer memory, 1/4 of the overall model is selected for the modeled region according to the symmetry of the engineering layout. In addition, only PW1 and PW2 wellbores with the same wellbore spacing were deemed as modeled wellbores, whereas PW3 was not considered. After grid mesh, the modeled region was divided into 33 grids in the x and y directions, with one grid of 10 m × 10 m, and a grid in the Z direction, representing the thickness of the coal seam of 6.3 m (Fig. 2(b)).

2.4 Key parameters and simulation schemes

Table 1 lists the parameters used for simulating CO_2-ECBM. The parameters were derived from relevant references (Fang et al., 2019a; Wang et al., 2022). As shown in Fig. 3, the fluid migration of gas-water two-phase was controlled by gas-water relative permeability characteristics (Fan et al., 2019). The existence of the water phase resulted in low effective permeability of the gas phase in the early stage of drainage and production, while during CO_2-ECBM, gas driving water also led to the decrease in effective permeability of the gas phase at the displacement front (Wang et al., 2022). The higher the water saturation, the more unfavorable the CH_4 recovery (Fan et al., 2019). Zhang et al. (2022) reported that the drainage and production levels should be increased to achieve a better displacement effect. The method involving initial draining, followed by injection, is selected in this work. Before injection, the three wellbores including the IW, underwent drainage and depressurization for

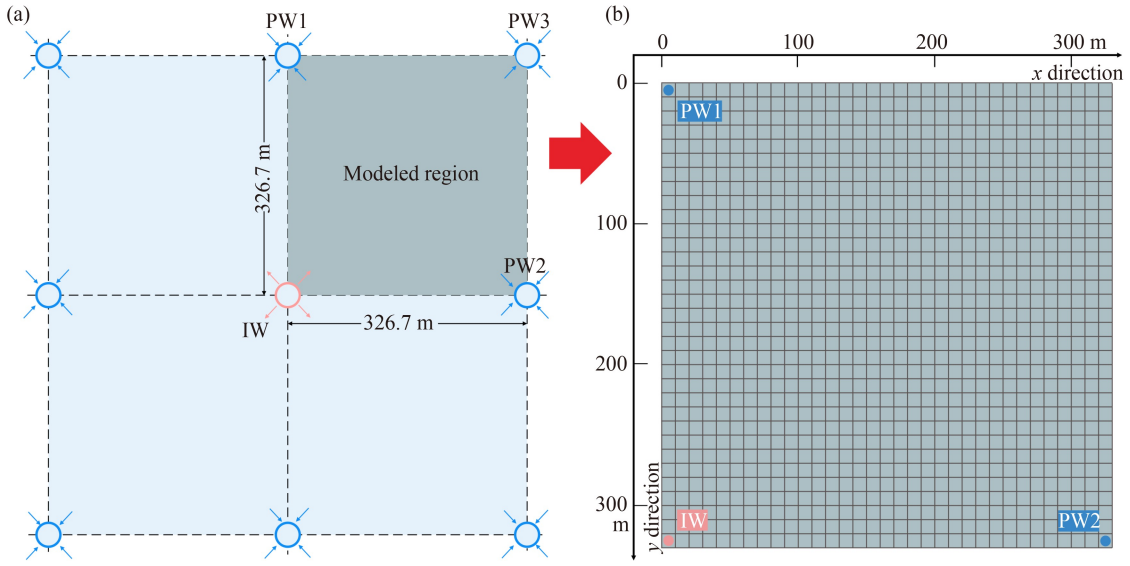

Fig. 2 Modeled region (a) and grid mesh (b).

Table 1 Key parameters used in the numerical study

Parameter	Value	Unit	Parameter	Value	Unit
Coal density	1.49×10^3	kg/m^3	Initial fracture permeability	0.5	mD
Temperature	23	°C	CO_2 Langmuir volume	48	m^3/t
Initial water saturation	100	%	CO_2 Langmuir pressure	0.75	MPa
CH_4 Initial content	14.5	m^3/t	CH_4 Langmuir volume	33	m^3/t
Initial porosity	0.035	–	CH_4 Langmuir pressure	2.23	MPa
Coal thickness	6.3	m	CH_4 dynamic viscosity	1.03×10^{-5}	Pa·s
Reservoir pressure	4300	kPa	CO_2 dynamic viscosity	1.38×10^{-5}	Pa·s

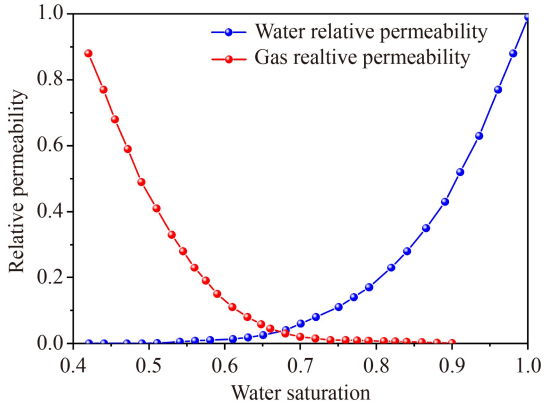

Fig. 3 Relative permeability characteristics for gas and water.

5 years. After drainage, CO_2 was injected into the reservoir at a pressure of 5 MPa. The simulation strategies are presented in Table 2. The permeability of K_y varied through values of 0.5, 2.5, and 5.0 mD. The anisotropy coefficient δ, equaling the ratio of K_x to K_y, was varied through values of 1.0, 5.0, and 10.0. Nine models were generated from the combination of K_y and δ.

3 Results and discussion

3.1 CH_4 output

Without injection, the yield rate of CH_4 decreased gradually over the drainage time, and the growth rate of CH_4 cumulative production slowed down. Within the CO_2 injection, as a result of the staged inhibition effect, the CH_4 production trend became complicated, due to which, the production rate did not increase under a few simulation schemes. However, the production rate of the producers increased significantly under most schemes, and the higher the permeability, the stronger the anisotropy, and the faster the gas production rate (Figs. 4(a)–4(c)). The peak CH_4 production rate could reach the values of 4278, 7770, and 13,653 m^3/d at the K_y values of 0.5, 2.5, and 5.0 mD, respectively. This is related to the efficient competitive sorption and displacement of CO_2 and CH_4, and the rapid migration of mixture fluid under the effect of high permeability and strong anisotropy.

As illustrated in Table 3, CH_4 cumulative production (after injection), CH_4 cumulative growth rate (after injection), hysteresis time, inhibition level, and inhibition

Table 2 Numerical simulation strategy

Serial number	Influencing factors	Value	Remark
Case 1	Permeability, K_y (mD)	0.5, 2.5, 5.0	A total of 9 models generated from the combination of K_y and δ
Case 2	Anisotropy coefficient, δ (K_x/K_y)	1.0, 5.0, 10.0	

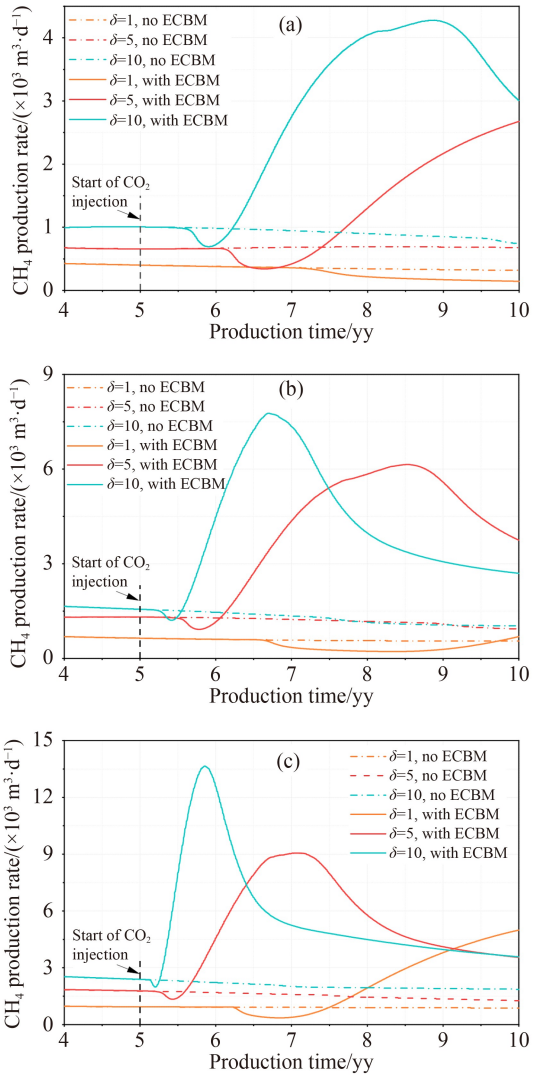

Fig. 4 Variations in CH_4 production rate over time under K_y of 0.5 (a), 2.5 (b), and 5.0 (c) mD.

time under different conditions are calculated. During CO_2 injection, the cumulative production of CH_4 dramatically increased with the increase in δ value, and had the values of 5.10×10^6 m^3, 7.55×10^6 m^3, and 10.30×10^6 m^3 for the K_y values of 0.5, 2.5, and 5.0 mD, respectively. In contrast to the isotropic condition, the cumulative production of CH_4 increased by 9.00-fold, 8.68-fold, and 1.85-fold, respectively. Remarkably, compared with non-injection, CO_2 injection failed to increase the CH_4 production rate effectively, and also reduced the cumulative growth rate of CH_4 by 21.02% and 26.28% during the running period under the isotropic conditions of the K_y values of 0.5 mD and 2.5 mD, respectively, while the cumulative growth rate of CH_4 could still attain the value of 117.17% under the K_y of 5.0 mD and homogeneous conditions. This indicates that relatively low permeable and isotropic reservoirs are not conducive to enhanced CH_4 recovery. However, with the increase in anisotropy coefficient, the negative trend effectively improved, and the maximal growth rates of CH_4 were found to be 205.89% and 234.32% for the K_y values of 0.5 mD and 2.5 mD, respectively. In addition, the improvement was significant at the K_y of 5 mD, with a maximum growth rate of 241.06%.

On the other hand, with the increase in K_y and δ, the hysteresis time, inhibition time, and inhibition level varied obviously. When K_y was varied through values of 0.5, 2.5, and 5.0 mD, the hysteresis time decreased from 731 days to 93 days, 574 days to 37 days, and 427 days to 5 days, with the reduced rates of 87.3%, 93.5%, and 98.8%, respectively. Meanwhile, the inhibition time decreased from more than 1091 days to 350 days, 1152 days to 162 days, and 501 days to 87 days, while the reduced rates were more than 67.9%, 85.9%, and 82.6%, respectively. The inhibition level changed from 36.9% to 11.50%, 43.7% to 8.30%, and 43.20% to 5.00%, with the reduced rates of more than 68.8%, 81.0%, and 88.4% under K_y of 0.5, 2.5, and 5.0 mD, respectively. In short, K_y and δ are negatively correlated with the hysteresis time, inhibition level, and duration, indicating that the coal reservoirs with relatively high permeability and strong anisotropy are favorable for accelerating CH_4 output.

However, the subsequent problem is that CO_2 tends to break through easily, which can lead to a large amount of CO_2 leakage that increases the cost of mixed-gas separation. Therefore, the threshold of CO_2 concentration is often used, and when the threshold is exceeded, shut-in measures are taken. CO_2 breakthrough and appointment of threshold inflict a profound impact on CH_4 recovery, CO_2 storage, and overall project income. At present, the common threshold consists of values of 10% and 20% (Balan and Gumrah, 2009; Luo et al., 2013). The following is a brief analysis based on the results presented in Table 4.

In contrast to the results presented in Table 3, considering CO_2 breakthrough and producers' shut-in, the cumulative production (after injection) illustrates two diverse trends in Table 4: under the condition of isotropic, and relatively low permeability and weak anisotropy, the cumulative production mostly remained unchanged. Secondly, under the condition of relatively high

Table 3 Statistical data of CH_4 output from PW2

K_y/mD	δ	CH_4 cumu. production/($\times10^6$ m^3)	Cumu. growth rate/%	Hysteresis duration/days	Inhibition level/%	Inhibition duration/days
0.5	1	0.51	−21.02	731	>36.90%	>1091
	5	2.24	81.06	217	23.90%	656
	10	5.10	205.89	93	11.50%	350
2.5	1	0.78	−26.28	574	43.70%	1152
	5	7.20	234.32	58	11.10%	327
	10	7.55	227.32	37	8.30%	162
5.0	1	3.61	117.17	427	43.20%	501
	5	9.52	241.06	30	9.70%	183
	10	10.30	174.49	5	5.00%	87

Table 4 Statistical data of CO_2 input, output, and storage of PW2

K_y/mD	δ	Threshold value/%	Breakthrough time [a]/yrs	Cumu. injection/ ($\times10^6$ m^3)	Cumu. production/ ($\times10^5$ m^3)	Cumu. storage [b]/ ($\times10^6$ m^3)	CH_4 Cumu. production [c]/ ($\times10^6$ m^3)
0.5	1	10/20	>5	11.91	0.00	11.91 (100.00%)	0.51 (0.51)
	5	10/20	>5	22.56	0.00	22.56 (100.00%)	2.24 (2.24)
	10	10	4.22	26.05	0.39	26.01 (99.85%)	4.07 (5.10)
		20	4.42	27.07	0.92	26.98 (99.66%)	4.38 (5.10)
2.5	1	10/20	>5	24.10	0.00	24.10 (100.00%)	0.78 (0.78)
	5	10	3.80	35.46	0.53	35.41 (99.85%)	5.13 (7.20)
		20	4.00	36.99	1.27	36.86 (99.66%)	5.56 (7.20)
	10	10	1.98	26.31	0.45	26.27 (99.83%)	3.22 (7.55)
		20	2.13	27.92	1.11	27.81 (99.60%)	3.60 (7.55)
5.0	1	10/20	>5	42.67	0.00	42.67 (100.00%)	3.61 (3.61)
	5	10	2.25	35.75	0.59	35.69 (99.83%)	4.41 (9.52)
		20	2.41	37.82	1.44	37.68 (99.62%)	4.90 (9.52)
	10	10	0.86	23.78	0.52	23.73 (99.78%)	2.19 (10.30)
		20	0.95	26.07	1.31	25.94 (99.50%)	2.64 (10.30)

Notes: a) More than 5 (> 5) years means no CO_2 breakthrough during the running period. b) The numbers before the brackets are CO_2 storage, and the ones within the brackets represent the CO_2 storage efficiency. c) The numbers before the brackets are the CH_4 cumulative production considering CO_2 breakthrough and shut-in, while those within the brackets are the CH_4 cumulative production without considering CO_2 breakthrough.

permeability, the cumulative production manifested a decline to different degrees.

For the K_y of 0.5 mD and δ of 10, the CH_4 cumulative production decreased from 5.10 × 10^6 m^3 to 4.07 × 10^6 m^3. For the K_y of 2.5 mD and δ of 5 and 10, the cumulative production dropped from 7.20 × 10^6 m^3 to 5.13 × 10^6 m^3, and 7.55 × 10^6 m^3 to 3.22 × 10^6 m^3, respectively. Additionally, for the K_y of 5.0 mD, and δ of 5 and 10, the cumulative production declined from 9.52 × 10^6 m^3 to 4.41 × 10^6 m^3 and 10.30 × 10^6 m^3 to 2.19 × 10^6 m^3, respectively (the threshold of CO_2 concentration was 10%). Among them, the decline rate augments with the increase in K_y and δ, with a minimum value of over 20.00% and a maximum value of 78.70%. Combined with the above findings, it can be inferred that, although the coal reservoirs with relatively high permeability and strong anisotropy are supportive to CH_4 replacement and displacement, large amounts of CH_4 cannot be produced once CO_2 breakthroughs and producers' shut-in are considered, thus resulting in a lower cumulative production of CH_4 than that expected.

Increasing the threshold of CO_2 breakthrough concentration from 10% to 20% is expected to mitigate the unfavorable trend. The measure not only prolongs the production time from 33 to 74 days, but also increases the cumulative production of CH_4 by 0.31 × 10^6–0.49 × 10^6 m^3. Nevertheless, while increasing the CH_4 production, this also increases the CO_2 production and diminishes the CO_2 sequestration volume.

3.2 CO_2 output and storage

With the increase in K_y and δ, the CO_2 breakthrough time decreased considerably (Table 4). For the K_y values of

0.5, 2.5, and 5.0 mD, the CO_2 breakthrough time decreased from more than 5 years (no breakthrough) to 4.22 years, over 5 years to 1.98 years and more than 5 years to 0.86 years, respectively. No CO_2 was produced, whereas the CO_2 storage efficiency was up to 100% under isotropic conditions. This indicates that isotropic conditions are favorable for CO_2 sequestration. Moreover, the cumulative injection and storage produced a significant positive correlation with K_y.

Figure 5 shows the variations of CO_2 cumulative injection under different conditions without considering CO_2 breakthrough. The cumulative injection of CO_2 increased with the increase of K_y and δ. However, considering the CO_2 breakthrough, the relationship presented diversity under anisotropic conditions (Table 4). For the K_y value of 0.5 mD, the CO_2 cumulative injection increased with the increase of δ. For the K_y value of 2.5 mD, the CO_2 cumulative injection first increased, and then, decreased with the increase of δ. For the K_y of 5.0 mD, the CO_2 cumulative injection decreased with the increase in δ. The analysis revealed that the reservoir permeability and anisotropy indicated two aspects in the process. For one thing, higher permeability and stronger anisotropy were beneficial to increasing the CO_2 injection, which is a positive effect. For another, higher permeability and stronger anisotropy led to significantly earlier breakthrough of CO_2 and premature producers shut-in, which is a negative effect. Therefore, for reservoirs with diverse permeability characteristics, it is necessary to rationally optimize the injection process to achieve the maximum benefit. The correlation also poses a similar variation trend between the CO_2 storage and K_y, and δ. It is worth noting that CO_2 storage efficiency changed slightly and remained at a high level (more than 99.00%).

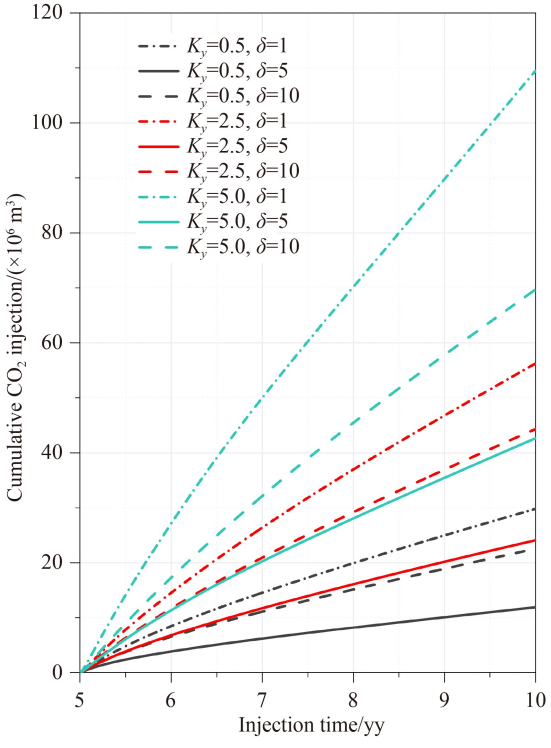

Fig. 5 Variations in CO_2 cumulative injection over time under different conditions.

Additionally, when the concentration threshold increased from 10% to 20%, the CO_2 cumulative injection increased by 1.02×10^6–2.29×10^6 m^3. The increment of CO_2 output was 0.53×10^5–0.85×10^5 m^3, which was 2.24–2.52 times that under the threshold of 10%. However, the CO_2 storage efficiency was still more than 99.00%. This indicates that appropriately increasing and maintaining the limit of CO_2 concentration contributes to CO_2 injection and CO_2 sequestration under the premise of relatively high storage efficiency. Certainly, the upper limit of CO_2 concentration might be increased further; however, the range will become beyond the scope of this paper, due to which, the author did not carry out an in-depth study.

3.3 Analysis of the staged inhibition process and the ideal displacing profile

In the process of primary drainage and pressure reduction, with the propagation of the depressurization cone, the water saturation in reservoirs continues to decrease, often remaining relatively low near wellbores and gradually increasing outwards. For the wellbore group with the injector and the producer, the water saturation is low near the wellbore and high between the wellbores.

Nevertheless, once gas injection began, the CO_2 could drive the residual fracture water in the nearby wellbores and between the wellbores to the producers, thus further reducing the saturation around the wellbores, increasing the saturation at the displacing front, and even forming the saturated-water bank. The increase in the fracture water saturation directly led to the decline of effective permeability of gas at the displacing front, which resulted in the drawdown of CH_4 yield, or more precisely, resulting in the inhibition effect on the CH_4 output (Wang et al., 2022). Furthermore, when abundant water was drained from the producers in a short time, this inhibition effect could disappear (Omotilewa et al., 2021), with obvious stage characteristics. However, most of the previous studies did not consider the effect of reservoir water, so the enhanced CH_4 recovery could come true quickly after CO_2 injection (Fan et al., 2018; Fang et al., 2019a, 2019b; Liu et al., 2020). Fan et al. (2019) found that water saturation had a certain influence on the production of gas and ignoring the impact of water results in an overestimation of the production of gas. The findings in Omotilewa et al. (2021) and Wang et al. (2022) were consistent with the results obtained in this work; however, the gas production in Wang et al. (2022)

might be underestimated due to the assumption of low-permeable homogeneous reservoir. The permeability in the real reservoir is anisotropic and heterogeneous, and this is beneficial to the seepage of fracture water, resulting in a weaker inhibition effect, as described earlier in the section.

The dynamic evolution of permeability, aroused by CO_2 adsorption-induced matrix swelling and CH_4 desorption-induced matrix shrinkage influenced the fluid flow. Although this is not considered in this work, according to some previous findings, with the progression of injection, the net swelling of the coal matrix occurred around the wellbores, resulting in a decrease in permeability, the amount of injected CO_2 and the production of CH_4 (Shi and Durucan, 2005; Durucan and Shi, 2009; Omotilewa et al., 2021). Of course, the increase in pore pressure can increase the fracture aperture, which is expected to alleviate the decrease in absolute permeability (Pan and Connell, 2012). However, combined with the matrix deformation and the change of pore pressure, the reservoir permeability still tended to decrease after CO_2 injection (Fang et al., 2019a). Therefore, it is speculated that the hysteresis time and inhibition time of producers may be prolonged, and the inhibition level may also be deepened.

The influence of free water on the production of CH_4 can also be qualitatively described by establishing the displacing profile. Both the theoretical and modeled studies indicated that, driven by CO_2, the residual fracture water and displaced CH_4 migrated to the producers, whereas the water affected the surrounding producers. Moreover, the displaced CH_4 influenced the producers and was extracted. Definitively, the CO_2 impacted the producers, and the concentration of CO_2 in the produced gas increased gradually. Accordingly, the CO_2-ECBM process displacing profile could be established (see Fig. 6), which consisted of CO_2 enriched bank, CO_2-CH_4 enriched bank, CH_4 enriched bank, and water enriched bank along the direction of fluid migration. The boundaries of these banks were not strictly and clearly defined, and their sizes and locations dynamically changed with the reservoir characteristics and injection process.

As illustrated in Fig. 6, remarkable discrepancies in the displacing profile of the dominant (the right side) and the non-dominant (the left side) seepage directions existed (sharing the same injector, the injection process was the same). With more efficient displacing process in the dominant directions, the CH_4 enriched bank was applied to the producer. Meanwhile, while in the non-dominant directions, the producer was still under the impact of water enriched bank. In other words, for the wellbores group with a single injector, the CH_4 output response of different producers was not synchronous, thus requiring accurate evaluation and scientific prediction to facilitate field operations.

However, due to the non-negligible heterogeneity and anisotropy of coal reservoirs and multifactor integrated control of output and storage, there was still a certain gap between the trial projects and the theoretical research, due to which, the displacing profile was only regarded as an ideal displacing profile.

3.4 Contrast of gas output behavior of different producers

The above results have pointed out that there exist

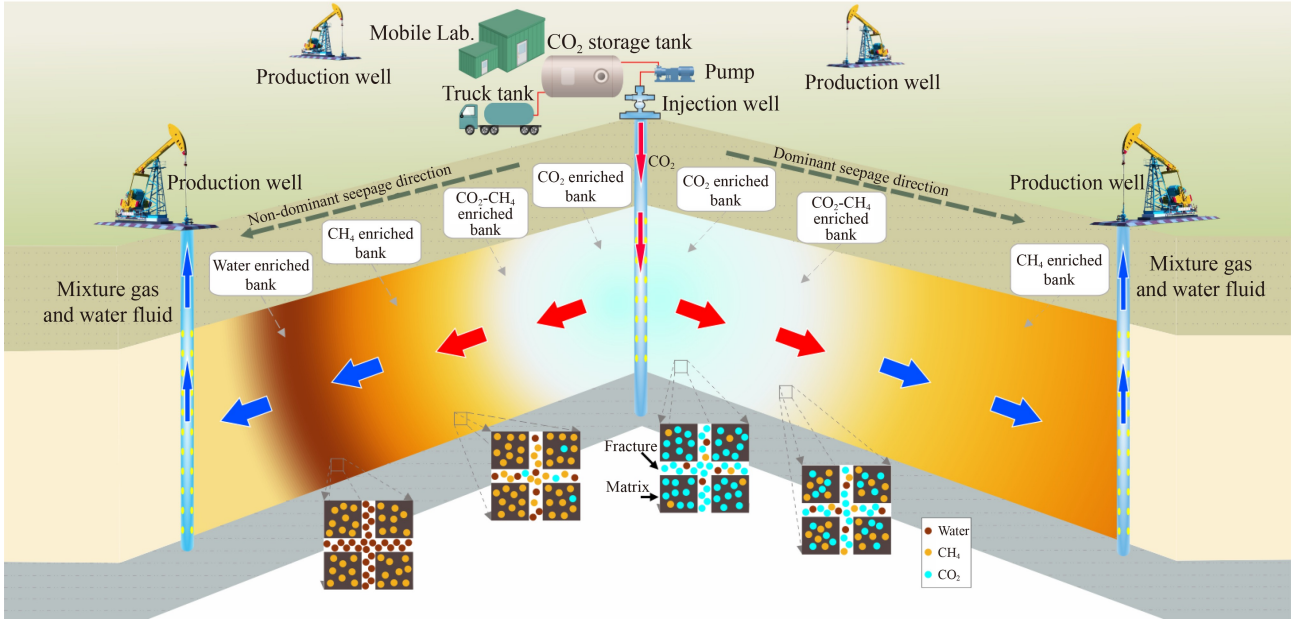

Fig. 6 Ideal displacing profile for CO_2-ECBM process.

differences in displacing profiles of different seepage directions and the gas output response of different producers is not synchronous. This section takes PW1 and PW2 as an example to conduct a comparative analysis and tries to observe the real gap to guide the field projects.

As shown in Fig. 2, the PW1 and PW2 possessed the same spacing with the injector and were in the non-dominant and dominant seepage directions, respectively. Figure 7 demonstrates the variations of CH_4 production rate and cumulative production in PW1 and PW2 with production time under the K_y value of 0.5 mD and different δ conditions. Under isotropic conditions, the CH_4 production rate and cumulative production of the two wellbores were almost the same. Under the anisotropic conditions, the CH_4 output of PW1 did not increase, and was prominently lower than that of the PW2. When the δ value was 5, the maximum CH_4 production rate of the PW2 reached the value of 2676 m^3/d, whereas the cumulative production was 2.24×10^6 m^3, which was 4.24 and 2.42 times the corresponding values for PW1, respectively. This difference increased with the increase in δ. For the δ value of 10, the maximum CH_4 production rate of PW2 was more than 4278 m^3/d, which was 4.96 times of the PW1. Besides, the cumulative production was 3.93 times that of the PW1. The cumulative production of PW2 (4.07×10^6 m^3) was 3.15 times higher than that of PW1 (1.29×10^6 m^3) during the running period, even when the CO_2 breakthrough and shut-in of PW2 were considered.

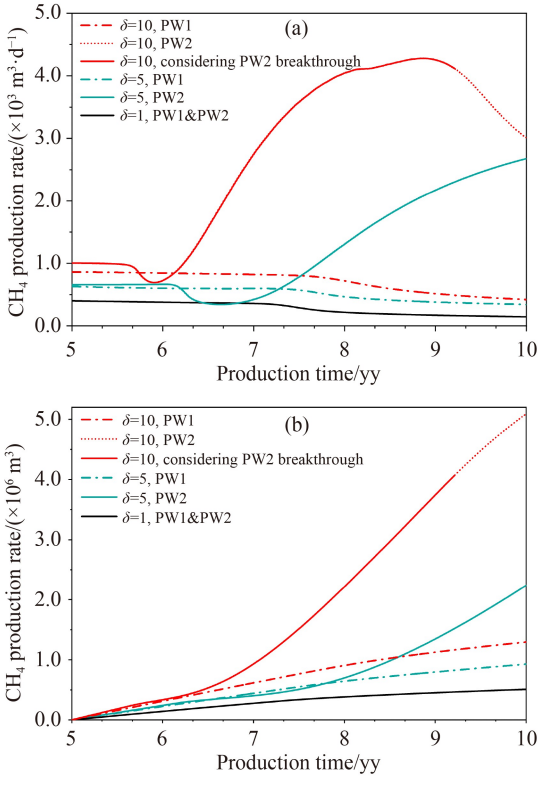

Fig. 7 Variations of CH_4 production rate (a) and cumulative production (b) in different producers.

Figure 8 illustrates the dynamic evolution of CH_4 in the matrix. After injection, considerable amounts of CH_4 were desorbed around the injector under the effect of competitive sorption and displacement, whereas the gas content of CH_4 in the displacing front markedly increased. With the lasting injection and extraction, the displacing front gradually propagated and effectively attacked the surrounding producers, which had a positive effect on the CH_4 output. However, with the increase in δ, the dominant direction emerged and the displacing front varied from circular to elliptic. The PW2 preferentially attained a CH_4 enriched bank. Although a great quantity of displaced CH_4 was also enriched in the area between IW and PW1, it was still unable to be effectively extracted from PW1 during the 5-year injection time. It can be expected that the situation will improve significantly with the continued operation. Therefore, to maximize the project certainty, it is necessary to identify the permeability heterogeneity and anisotropy characteristics of coal reservoir before the implementation of CO_2-ECBM. Based upon these results, potential prediction of enhanced CH_4 recovery and the optimization of CO_2 injection process should be performed.

4 Conclusions

1) Low-permeable or weak-anisotropic reservoirs were not conducive to enhanced CH_4 recovery owing to long inhibition time (> 1091 days) and high inhibition level (> 36.9%). As the permeability and anisotropy increased, due to the accelerated seepage of free water, the hysteresis time and inhibition time could decrease to as short as 5 days and 87 days, respectively, whereas the inhibition level could weaken to as low as 5.00%. Moreover, the CH_4 output and CO_2 injection could increase significantly.

2) Nevertheless, high permeability and strong anisotropy easily induced CO_2 breakthrough, resulting in lower CH_4 production, CO_2 injection and storage than expected. While maintaining the high efficiency of CO_2 storage (> 99%), upregulating CO_2 breakthrough concentration from 10% to 20% might ease the unfavorable trend.

3) Along the direction of fluid flow, the ideal displacing profile consisted of CO_2 enriched bank, CO_2 and CH_4 mixed bank, CH_4 enriched bank, and water enriched bank, whereas a remarkable gap in the displacement profiles of the dominant and the non-dominant seepage directions was observed.

4) The potential of CH_4 output might vary greatly among different wellbores. The producers along the dominant seepage direction held more potential for CH_4

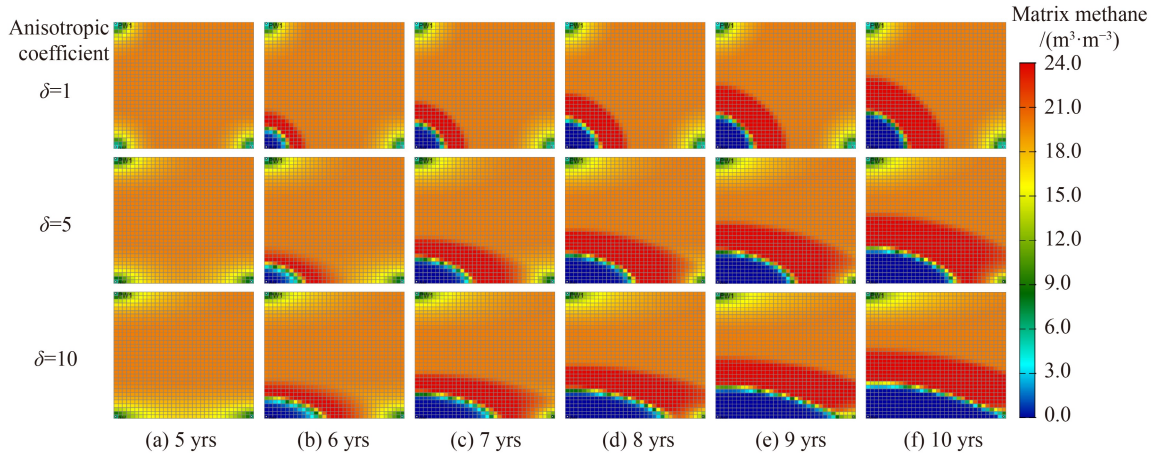

Fig. 8 Dynamic evolution of CH_4 content in different conditions.

recovery in the short-term, while those along the non-dominant seepage direction avoided becoming invalid only if a long-time injection measure was taken for the injectors.

Acknowledgments This work was funded by the National Natural Science Foundation of China (Grant No. 42141012), the National Key R&D Program of China (No. 2018YFB0605600), and the Priority Academic Program Development of Jiangsu Higher Education Institutions (PAPD).

Competing interests The authors declare that they have no competing interests.

References

Balan H O, Gumrah F (2009). Assessment of shrinkage–swelling influences in coal seams using rank-dependent physical coal properties. Int J Coal Geol, 77(1–2): 203–213

Bui M, Adjiman C S, Bardow A, Anthony E J, Boston A, Brown S, Fennell P S, Fuss S, Galindo A, Hackett L A, Hallett J P, Herzog H J, Jackson G, Kemper J, Krevor S, Maitland G C, Matuszewski M, Metcalfe I S, Petit C, Puxty G, Reimer J, Reiner D M, Rubin E S, Scott S A, Shah N, Smit B, Trusler J P M, Webley P, Wilcox J, Mac Dowell N (2018). Carbon capture and storage (CCS): the way forward. Energy Environ Sci, 11(5): 1062–1176

Connell L D, Detournay C (2009). Coupled flow and geomechanical processes during enhanced coal seam methane recovery through CO_2 sequestration. Int J Coal Geol, 77(1–2): 222–233

Du Y, Sang S, Pan Z, Wang W, Liu S, Fu C, Zhao Y, Zhang J (2019). Experimental study of supercritical CO_2–H_2O-coal interactions and the effect on coal permeability. Fuel, 253: 369–382

Durucan S, Shi J Q (2009). Improving the CO_2 well injectivity and enhanced coalbed methane production performance in coal seams. Int J Coal Geol, 77(1–2): 214–221

Fan C, Elsworth D, Li S, Zhou L, Yang Z, Song Y (2019). Thermo-hydro-mechanical-chemical couplings controlling CH_4 production and CO_2 sequestration in enhanced coalbed methane recovery. Energy, 173: 1054–1077

Fan J L, Xu M, Wei S, Shen S, Diao Y, Zhang X (2021). Carbon reduction potential of China's coal-fired power plants based on a CCUS source-sink matching model. Resour Conserv Recycling, 168: 105320

Fan Y, Deng C, Zhang X, Li F, Wang X, Qiao L (2018). Numerical study of CO_2-enhanced coalbed methane recovery. Int J Greenh Gas Control, 76: 12–23

Fang H, Sang S, Liu S (2019a). Establishment of dynamic permeability model of coal reservoir and its numerical simulation during the CO_2-ECBM process. J Petrol Sci Eng, 179: 885–898

Fang H, Sang S, Liu S, Liu S (2019b). Experimental simulation of replacing and displacing CH_4 by injecting supercritical CO_2 and its geological significance. Int J Greenh Gas Control, 81: 115–125

Godec M, Koperna G, Gale J (2014). CO_2-ECBM: a review of its status and global potential. Energy Procedia, 63: 5858–5869

Hasan M M F, First E L, Boukouvala F, Floudas C A (2015). A multi-scale framework for CO_2 capture, utilization, and sequestration: CCUS and CCU. Comput Chem Eng, 81: 2–21

Jiang K, Ashworth P, Zhang S, Liang X, Sun Y, Angus D (2020). China's carbon capture, utilization and storage (CCUS) policy: a critical review. Renew Sustain Energy Rev, 119: 109601

Kang J, Fu X, Li X, Liang S (2019). Nitrogen injection to enhance methane and water production: an experimental study using the LF-NMR relaxation method. Int J Coal Geol, 211: 103228

Kumar H, Elsworth D, Mathews J, Liu J, Pone D (2014). Effect of CO_2 injection on heterogeneously permeable coalbed reservoirs. Fuel, 135: 509–521

Leonzio G, Foscolo P U, Zondervan E (2019). An outlook towards 2030: optimization and design of a CCUS supply chain in Germany. Comput Chem Eng, 125: 499–513

Li Q, Chen Z A, Zhang J T, Liu L C, Li X C, Jia L (2016). Positioning and revision of CCUS technology development in China. Int J Greenh Gas Control, 46: 282–293

Li Y, Wang Y, Wang J, Pan Z (2020). Variation in permeability during CO_2–CH_4 displacement in coal seams: part 1 – experimental insights. Fuel, 263: 116666

Liu S, Fang H, Sang S, Ashutosh T, Wu J, Zhang S, Zhang B (2020). CO_2 injectability and CH_4 recovery of the engineering test in Qinshui Basin, China based on numerical simulation. Int J Greenh Gas Control, 95: 102980

Liu T, Lin B, Yang W (2017). Impact of matrix-fracture interactions on coal permeability: model development and analysis. Fuel, 207: 522–532

L'Orange Seigo S, Dohle S, Siegrist M (2014). Public perception of carbon capture and storage (CCS): a review. Renew Sustain Energy Rev, 38: 848–863

Luo F, Xu R N, Jiang P X (2013). Numerical investigation of the influence of vertical permeability heterogeneity in stratified formation and of injection/production well perforation placement on CO_2 geological storage with enhanced CH_4 recovery. Appl Energy, 102: 1314–1323

Mazumder S, Wolf K H (2008). Differential swelling and permeability change of coal in response to CO_2 injection for ECBM. Int J Coal Geol, 74(2): 123–138

Omotilewa O J, Panja P, Vega-Ortiz C, McLennan J (2021). Evaluation of enhanced coalbed methane recovery and carbon dioxide sequestration potential in high volatile bituminous coal. J Nat Gas Sci Eng, 91: 103979

Pan Z, Connell L D (2012). Modelling permeability for coal reservoirs: a review of analytical models and testing data. Int J Coal Geol, 92: 1–44

Pan Z, Connell L D (2011). Modelling of anisotropic coal swelling and its impact on permeability behaviour for primary and enhanced coalbed methane recovery. Int J Coal Geol, 85(3–4): 257–267

Paul G W, Sawyer W K, Dean R H (1990). Validation of 3D coalbed simulators. In: SPE Annual Technical Conference and Exhibition, New Orleans, Louisiana, SPE-20733-MS

Reeves S, Pekot L (2001). Advanced reservoir modeling in desorption-controlled reservoirs. In: SPE Rocky Mountain Petroleum Technology Conference, Keystone, Colorado, SPE-71090-MS

Sang S X (2018). Research review on technical effectiveness of CO_2 geological storage and enhanced coalbed methane recovery. Coal Geol Explor, 46: 1–9 (in Chinese)

Sang S X, Wang R, Zhou X Z, Huang H Z, Liu S Q, Han S J (2021). Review on carbon neutralization associated with coal geology. Coal Geol Explor, 49(1): 1–11 (in Chinese)

Sawyer W K, Paul G W, Schraufnagel R A (1990). Development and application of a 3-D coalbed simulator. In: Annual Technical Meeting, Petroleum Society of Canada, Calgary, Alberta

Shi J Q, Durucan S (2005). A model for changes in coalbed permeability during primary and enhanced methane, recovery. SPE Reservoir Eval Eng, 8(4): 291–299

Sun L, Chen W (2022). Impact of carbon tax on CCUS source-sink matching: finding from the improved ChinaCCS DSS. J Clean Prod, 333: 130027

Sun Z, Shi J, Wang K, Miao Y, Zhang T, Feng D, Sun F, Wang S, Han S, Li X (2018a). The gas-water two phase flow behavior in low-permeability CBM reservoirs with multiple mechanisms coupling. J Nat Gas Sci Eng, 52: 82–93

Sun Z, Shi J, Zhang T, Wu K, Feng D, Sun F, Huang L, Hou C, Li X (2018b). A fully-coupled semi-analytical model for effective gas/water phase permeability during coal-bed methane production. Fuel, 223: 44–52

Tang H, Zhang S, Chen W (2021). Assessing representative CCUS layouts for China's power sector toward carbon neutrality. Environ Sci Technol, 55(16): 11225–11235

Tapia J F D, Lee J Y, Ooi R E H, Foo D C Y, Tan R R (2018). A review of optimization and decision-making models for the planning of CO_2 capture, utilization and storage (CCUS) systems. Sustain Product Consump, 13: 1–15

Vishal V, Mahanta B, Pradhan S P, Singh T N, Ranjith P G (2018). Simulation of CO_2 enhanced coalbed methane recovery in Jharia coalfields, India. Energy, 159: 1185–1194

Vishal V, Singh L, Pradhan S P, Singh T N, Ranjith P G (2013). Numerical modeling of Gondwana coal seams in India as coalbed methane reservoirs substituted for carbon dioxide sequestration. Energy, 49: 384–394

Wang C, Zhang J, Zang Y, Zhong R, Wang J, Wu Y, Jiang Y, Chen Z (2021). Time-dependent coal permeability: impact of gas transport from coal cleats to matrices. J Nat Gas Sci Eng, 88: 103806

Wang Z, Sang S, Zhou X, Liu X (2022). Numerical study on CO_2 sequestration in low-permeability coal reservoirs to enhance CH_4 recovery: gas driving water and staged inhibition on CH_4 output. J Petrol Sci Eng, 214: 110478

Warren J E, Root P J (1963). The behavior of naturally fractured reservoirs. Soc Pet Eng J, 3(3): 245–255

Wei C, Qin Y, Fu X, Shen J (2015). Coalbed Methane Reservoir Modeling. Beijing: Science Press

White C M, Smith D H, Jones K L, Goodman A L, Jikich S A, LaCount R B, DuBose S B, Ozdemir E, Morsi B I, Schroeder K T (2005). Sequestration of carbon dioxide in coal with enhanced coalbed methane recovery−a review. Energy Fuels, 19(3): 659–724

Xu S, Dai S (2021). CCUS as a second-best choice for China's carbon neutrality: an institutional analysis. Clim Policy, 21(7): 927–938

Xue D J, Zhou H W, Liu Y T, Deng L S, Zhang L (2018). Study of drainage and percolation of nitrogen-water flooding in tight coal by NMR imaging. Rock Mech Rock Eng, 51(11): 3421–3437

Yu S, Horing J, Liu Q, Dahowski R, Davidson C, Edmonds J, Liu B, Mcjeon H, McLeod J, Patel P, Clarke L (2019). CCUS in China's mitigation strategy: insights from integrated assessment modeling. Int J Greenh Gas Control, 84: 204–218

Zhang S, Tang S, Zhang S, Wang J (2022). Simulation and evaluation of enhanced coalbed methane recovery by CO_2 storage in coal reservoirs with different drainage and production levels. J China Coal Soc, 47: 1275–1285 (in Chinese)

Zhang X, Ranjith P G (2019). Experimental investigation of effects of CO_2 injection on enhanced methane recovery in coal seam reservoirs. J CO_2 Utilization, 33: 394–404

Zhao Y, Lin B, Liu T (2020). Thermo-hydro-mechanical couplings controlling gas migration in heterogeneous and elastically-deformed coal. Comput Geotech, 123: 103570